Available online at www.sciencedirect.com
SCIENCE DIRECT®
Chemical Physics 308 (2005) 93–102
Chemical Physics
www.elsevier.com/locate/chemphys

Absorption and emission spectroscopic characterization of $Ir(ppy)_3$

W. Holzer [a], A. Penzkofer [a,*], T. Tsuboi [b]

[a] *Institut II – Experimentelle und Angewandte Physik, Universität Regensburg, Universitätsstrasse 31, D-93053 Regensburg, Germany*
[b] *Faculty of Engineering, Kyoto Sangyo University, Kamigamo, Kita-ku, Kyoto 603-8555, Japan*

Received 29 July 2004; accepted 30 July 2004
Available online 6 October 2004

Abstract

The absorption and emission spectroscopic behaviour of cyclometalated *fac*-tris(2-phenylpyridine) iridium(III) [$Ir(ppy)_3$] is studied at room temperature. Liquid solutions, doped films, and neat films are investigated. The absorption cross-section spectra including singlet–triplet absorption, the triplet–singlet stimulated emission cross-section spectra, the phosphorescence quantum distributions, the phosphorescence quantum yields and the phosphorescence signal decays are determined. In neat films fluorescence self-quenching occurs, in diluted solid solution (polystyrene and dicarbazole-biphenyl films) as well as deaerated liquid solution (toluene) high phosphorescence quantum yields are obtained, and in air-saturated liquid solutions (chloroform, toluene, tetrahydrofuran) the phosphorescence efficiency is reduced by triplet oxygen quenching. At intense short-pulse laser excitation the phosphorescence lifetime is shortened by triplet–triplet annihilation. No amplification of spontaneous emission in the phosphorescence spectral region was observed indicating higher excited-state absorption than stimulated emission.

Keywords: $Ir(ppy)_3$; Organometallic complex; MLCT-complex; Doped film; Neat film; Phosphorescence quantum yield; Phosphorescence lifetime; Singlet–triplet absorption; Stimulated emission cross-section; Triplet–triplet annihilation; Amplified spontaneous emission

1. Introduction

Phosphorescent materials like lanthanide complexes [1], purely organic phosphors [2], and organometallic phosphors [3] gain importance in organic light emitting diodes (OLEDs) [4] because of higher potential efficiency than singlet emitters. In organic materials one quarter of electrons is excited to the singlet system and three quarters are excited to the triplet system by electrical pumping. In phosphorescent materials strong intersystem-crossing transfers the singlet excited molecules to the triplet system, resulting in an accumulation of all excited molecules in the triplet system. In the group of organometallic complexes, especially porphyrine platinum complexes such as platinium octaethylporphyrin (PtOEP) [5–10] and phenylpyridine iridium complexes such as $Ir(ppy)_3$ [11–25] are the most widely used phosphorescent OLED materials.

In this paper we undertake an absorption and emission spectroscopic characterisation of *fac*-tris(2-phenylpyridyl)Ir(III) [$Ir(ppy)_3$] at room temperature in neat film form, in liquid organic solution (solvents: chloroform, toluene, and tetrahydrofuran), in a polystyrene matrix, and in a 4,4′-*N*,*N*′-dicarbazole-biphenyl (CBP) film. CBP is used in OLEDs as hole-transport material [4]. The fluorescence spectrum and phosphorescence spectrum of CBP is found in [26] and [27], respectively. The structural formulae of $Ir(ppy)_3$, CBP, and polystyrene are shown in Fig. 1. Information on the synthesis of $Ir(ppy)_3$ is found in [28,29]. Some optical absorption [29–34] and luminescence spectroscopic characterisation [29–36] of $Ir(ppy)_3$ is found in the literature. Spectral electroluminescence studies [4,11,12,14,27,33] and

* Corresponding author. Tel.: +49 941 943 2107; fax: +49 941 943 2754.
E-mail address: alfons.penzkofer@physik.uni-regensburg.de (A. Penzkofer).

0301-0104/$ - see front matter © 2004 Elsevier B.V. All rights reserved.
doi:10.1016/j.chemphys.2004.07.051

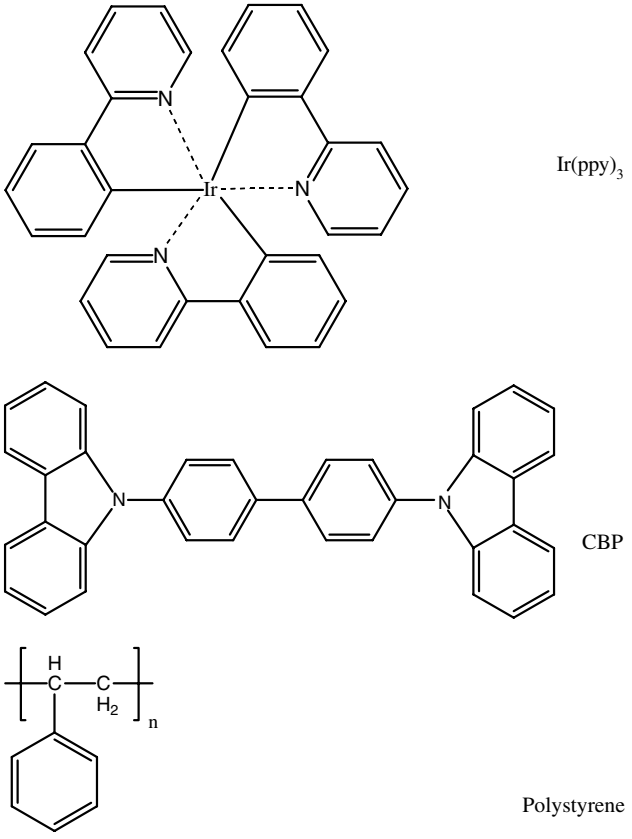

Fig. 1. Structural formulae of *fac*-tris(2-phenylpyridyl)Ir(III) [Ir(ppy)$_3$] (molar mass $M_m = 654.79$ g mol^{-1}), 4,4′-*N*,*N*′-dicarbazole-biphenyl (CBP, $M_m = 484.6$ g mol^{-1}), and polystyrene (molar mass of repeat unit $M_{RU} = 104.15$ g mol^{-1}, average degree of polymerisation $n \approx 430$).

temporal electroluminescence studies [27,36] were performed on OLED structures. Theoretical studies on the ground state and excited electronic states of cyclometalated phenylpyridine Ir(III) complexes have been carried out using density functional theory [37]. The long-wavelength absorption and the luminescence emission are understood as triplet MLCT (metal-to-ligand-charge-transfer) absorption and emission (phosphorescence) enhanced by heavy metal spin–orbit coupling [29,33,34,37].

2. Experimental

The metal complex Ir(ppy)$_3$ was purchased from H. W. Sands Corp., Jupiter, FL, USA. CBP was delivered by SynTec GmbH, Wolfen, Germany. Polystyrene (PS, molar mass 45,000 g mol^{-1}) and the solvents chloroform, toluene and tetrahydrofuran (THF) were purchased from Aldrich Co., Germany. All compounds were used as supplied without further purification. A 65 nm thick Ir(ppy)$_3$ neat film on a quartz glass substrate was provided by Pioneer Co. Japan. It was prepared by vapour deposition.

The Ir(ppy)$_3$/CBP and the Ir(ppy)$_3$/PS films are prepared by spin-coating the appropriate solutions on optical glass substrates. Both the solutions and the substrates are heated up to 80 °C for the spin coating. The films containing 7.9 wt% Ir(ppy)$_3$ in CBP are prepared by dissolving 3.16 mg Ir(ppy)$_3$ and 36.64 mg CBP in 1 ml THF, and spin-coating the solution on the heated substrate at a speed of 1600 rpm. The Ir(ppy)$_3$/PS films are made by spin coating the solutions on the heated substrate at a speed of 2000 rpm. For the films containing 1 wt% Ir(ppy)$_3$ there are dissolved 4 mg Ir(ppy)$_3$ and 396 mg PS are dissolved in 1 mg THF, for the films containing 4 wt% Ir(ppy)$_3$ there are dissolved 8.8 mg Ir(ppy)$_3$ and 211.2 mg PS are dissolved in 1 mg THF, while for the films containing 8 wt% Ir(ppy)$_3$ there are dissolved 6.4 mg Ir(ppy)$_3$ and 73.6 mg PS are dissolved in 1 mg THF.

Absorption cross-section spectra of diluted Ir(ppy)$_3$ are derived from transmission measurements with a commercial spectrophotometer (Beckman type ACTA M IV). The optical constants (absorption coefficient spectrum and refractive index spectrum) of Ir(ppy)$_3$ neat films and of Ir(ppy)$_3$ doped CBP films are determined from transmittance and reflectance measurements employing the Fresnel equations for parameter extraction [38–40].

The phosphorescence quantum distributions, $E_P(\lambda)$, are determined with a self-assembled fluorimeter in front-face collection arrangement [41,42]. The samples are exited at the wavelength $\lambda = 365$ nm with a mercury high-pressure lamp. For absolute calibration the dye quinine sulphate dihydrate (from Aldrich) dissolved in 1 N aqueous H_2SO_4 is used as reference (fluorescence quantum yield $\phi_F(C) = 0.546/[1 + 14.5C]$, where C is the dye concentration in mol dm^{-3} [43]). The phosphorescence quantum yield is given by $\phi_P = \int E_P(\lambda)\,d\lambda$. The fluorescence efficiency of Ir(ppy)$_3$ in toluene was determined under air saturated conditions as delivered and after de-aeration by nitrogen bubbling for 6 h.

The temporal luminescence behaviour is studied by picosecond laser pulse excitation using a mode-locked and frequency doubled ruby laser system (wavelength $\lambda_L = 347.15$ nm, duration $\Delta t_L = 35$ ps) [44] and emission detection with a fast micro-channel-plate photomultiplier (Hamamatsu type R1564U-01) and a fast real-time digital oscilloscope (LeCroy type 9362). Ir(ppy)$_3$ in deaerated toluene solution is studied by picosecond pulse excitation ($\Delta t_L \approx 4$ ps) at $\lambda_L = 401$ nm (second harmonic of Ti:sapphire laser Hurricane from Spectra-Physics). In the case of single-exponential decay the 1/*e* phosphorescence lifetime, τ_P, is extracted from the decay, and the radiative lifetime is determined by $\tau_{rad} = \tau_P/\phi_P$.

The stimulated emission cross-section spectrum is determined from the radiative lifetime, τ_{rad}, and the phosphorescence quantum distribution, $E_P(\lambda)$, by [45,46]

$$\sigma_{em}(\lambda) = \frac{\lambda^4}{8\pi n_P^2 c_0 \tau_{rad}} \frac{E_P(\lambda)}{\int_{em} E_P(\lambda')\,d\lambda'}, \quad (1)$$

where n_P is the mean refractive index in the phosphorescence region, c_0 is the vacuum light velocity. The integral extends over the phosphorescence emission region em. The radiative lifetime is related to the absorption strength of the relevant transition by the Strickler–Berg formula [47,48]

$$\tau_{rad}^{-1} = \frac{g_A}{g_P} \frac{8\pi c_0 n_P^3}{n_A} \frac{\int_{em} E_P(\lambda)\,d\lambda}{\int_{em} E_P(\lambda)\lambda^3\,d\lambda} \int_{abs} \frac{\sigma_a(\lambda)}{\lambda}\,d\lambda, \quad (2)$$

where g_A is the statistical weight of the singlet ground-state of the S_0–T_1 absorption transition ($g_A = 1$), and g_P is the statistical weight of the triplet state of the T_1–S_0 phosphorescence transition ($g_P = 3$). n_A is the mean refractive index in the S_0–T_1 absorption region. $\sigma_a(\lambda)$ is the absorption cross-section of the S_0–T_1 transition. The absorption integral extends over the S_0–T_1 absorption region abs. Eq. (2) will be used below to separate out the absorption cross-section spectrum of the lowest singlet–triplet transition (responsible for phosphorescence emission) from the complete absorption cross-section spectrum with the aid of the mirror symmetry relation between absorption and emission of a vibronic transition.

3. Results

In Fig. 2(a) the absorption cross-section spectra are shown of the hosts CBP dissolved in THF and of polystyrene dissolved in cyclohexane. Above 370 nm (CBP) and above 310 nm (PS) these hosts do not influence the absorption of the $Ir(ppy)_3$ guest molecules. The transmissions of the applied liquid solvents chloroform, THF, and toluene are displayed in Fig. 2(b) (cell thickness 1 cm) in order to see the transparency regions.

The absorption coefficient spectrum, $\alpha(\lambda)$, and the refractive index spectrum, $n(\lambda)$, of a 65 nm thick neat film of $Ir(ppy)_3$ on a quartz glass substrate is shown in Fig. 3. For $\lambda > 340$ nm the α and n values are determined by nearly normal incidence transmittance and reflectance measurements and Fresnel equation data analysis [38,39], while below 340 nm the absorption coefficient spectrum is determined by transmission measurement. Absorption shoulders and absorption peaks are found at 490, 460, 410, 380, 355, 287, and 245 nm. In the displayed wavelength region the refractive index dispersion is governed by the absorption peak around 380 nm. In Fig. 3(b) additionally the refractive index spectrum of CBP is displayed (dashed line).

The absorption cross-section spectra of $Ir(ppy)_3$ in chloroform, THF, and toluene are shown in Fig. 4. They are practically the same for the three solvents. The

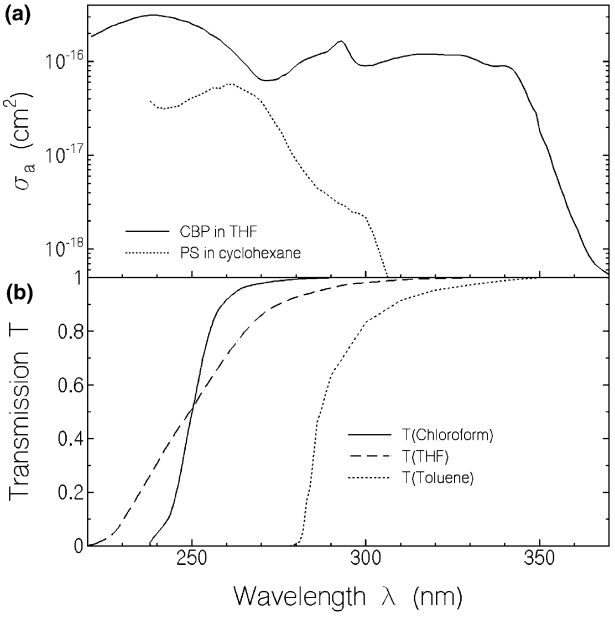

Fig. 2. (a) Absorption cross-section spectra of CBP dissolved in THF, and of polystyrene dissolved in cyclohexane. (b) Transmission spectra of chloroform, THF, and toluene. The sample thickness is 1 cm.

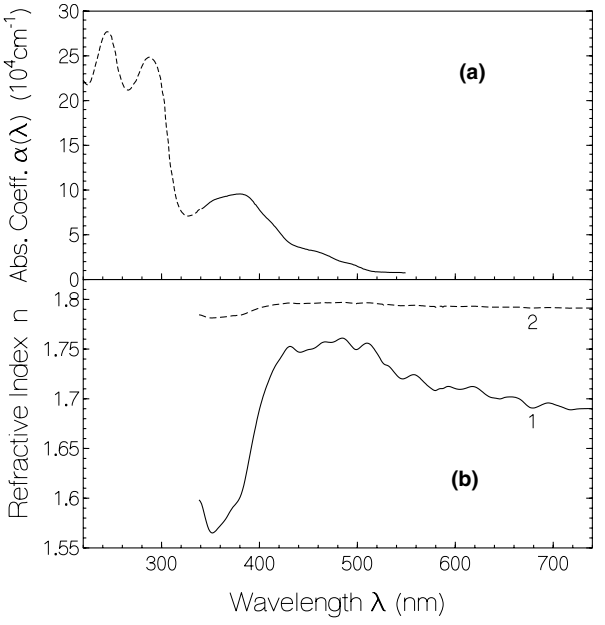

Fig. 3. (a) Absorption coefficient spectrum, $\alpha(\lambda)$, of $Ir(ppy)_3$, and (b) refractive index spectra, $n(\lambda)$, of (1) $Ir(ppy)_3$ and (2) CBP with 7.9 wt% $Ir(ppy)_3$.

absorption cross-section spectrum of the neat film is included. It is calibrated to the toluene solution spectrum by equating the absorption cross-section integrals for $\lambda \geqslant 340$ nm. The neat film spectrum is somewhat flattened compared to the solution spectra.

In Fig. 4 the stimulated emission cross-section spectra of $Ir(ppy)_3$ in chloroform, THF, and toluene are included. They are calculated by use of Eq. (1) from the phosphorescence quantum distributions and the

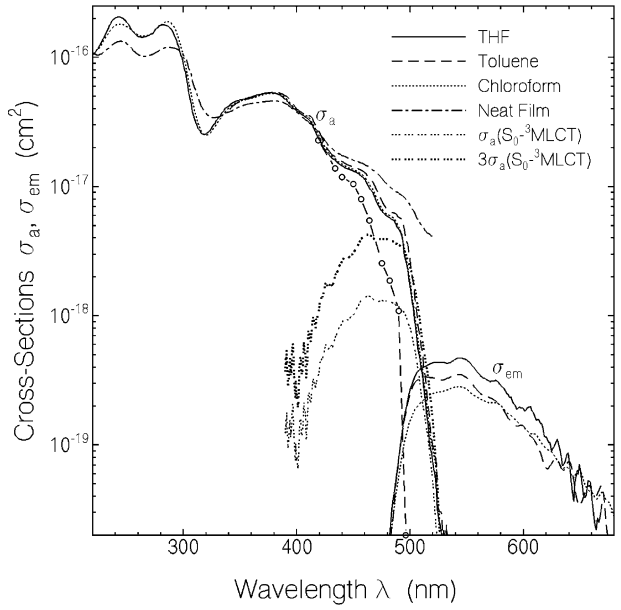

Fig. 4. Absorption cross-section spectra, $\sigma_a(\lambda)$, and stimulated emission cross-section spectra, $\sigma_{em}(\lambda)$, of $Ir(ppy)_3$ in THF, toluene, and chloroform at room temperature. The absorption spectrum of the neat $Ir(ppy)_3$ film is included (adjusted to have the same absorption cross-section integral for $\lambda > 340$ nm as the toluene solution). Thin triple-dotted curve, expected S_0–T_1 triplet absorption spectrum of $Ir(ppy)_3$ in THF. Thick triple-dotted curve, expected absorption cross-section spectrum of $Ir(ppy)_3$ in THF for the transitions from S_0 to T_1, T_2, and T_3 [37]. Line connected open circles, absorption spectrum of $Ir(ppy)_3$ in THF without the three lowest triplet contributions.

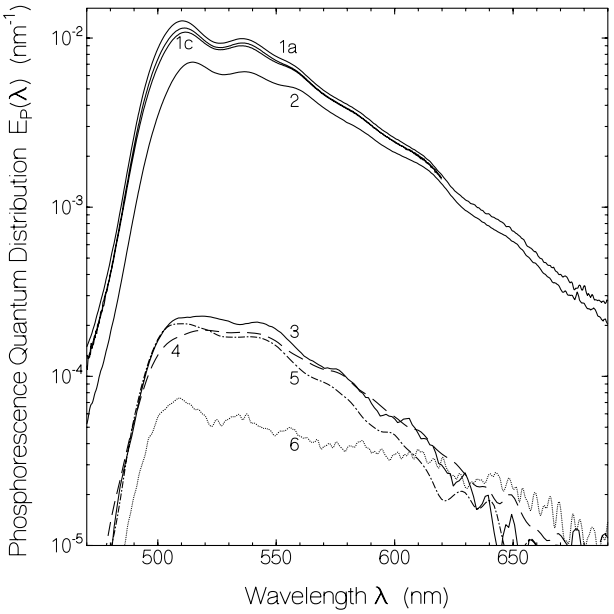

Fig. 5. Phosphorescence quantum distributions of $Ir(ppy)_3$ in different hosts. Curves 1a, 1 wt% in PS; 1b, 4 wt% in PS; 1c, 8 wt% in PS; 2, 7.9 wt% in CBP; 3, 1.8×10^{-4} M in THF; 4, 2.7×10^{-4} M in chloroform; 5, 2.1×10^{-4} M in toluene; 6, neat film.

radiative phosphorescence lifetimes (see below). These stimulated emission cross-section spectra are due to the T_1–S_0 transition. For the THF solution the corresponding S_0–T_1 absorption cross-section spectrum is shown by the thin triple-dotted curve. It is calculated by use of Eq. (2) and assuming mirror symmetry to the T_1–S_0 emission spectrum with image plane at $\lambda = 500$ nm. The S_0–T_1 absorption cross-section integral is a factor of three larger than the T_1–S_0 stimulated emission cross-section integral because of the threefold triplet degeneracy (statistical weight 3) [49].

The determined phosphorescence quantum distributions of $Ir(ppy)_3$ in the solid hosts polystyrene (1, 4, 8 wt%), CBP (7.9 wt%), the as delivered solvents THF (concentration $C = 1.8 \times 10^{-4}$ mol dm^{-3}), chloroform ($C = 2.7 \times 10^{-4}$ mol dm^{-3}), toluene ($C = 2.1 \times 10^{-4}$ mol dm^{-3}), and of the $Ir(ppy)_3$ neat film (thickness 65 nm) are shown in Fig. 5. The spectral shapes of the quantum distributions in solid and liquid solution are similar. A vibronic structure is resolved. For the neat film the distribution is broadened and less structured. The fluorescence quantum distribution of $Ir(ppy)_3$ in the de-aerated toluene solution (curve not shown) is a factor of 45 higher than in as delivered air saturated toluene. The phosphorescence efficiency decreases from solid solution and de-aerated toluene solution to air-saturated liquid solution to neat film. The determined phosphorescence quantum yields, $\phi_P = \int E_P(\lambda)\,d\lambda$, are listed in Table 1 together with the involved average refractive indices, n_A and n_P and the applied film and cell thicknesses, d.

Phosphorescence signal decay curves are displayed in Figs. 6 and 7. In the air saturated liquid solutions (Fig. 6) and in the de-aerated toluene solution (curve 1 in Fig. 7) single-exponential phosphorescence decays are observed. The phosphorescence lifetimes, τ_P, together with the radiative lifetimes, $\tau_{rad} = \tau_P/\phi_P$, are listed in Table 1. For the neat film fast non-exponential phosphorescence decay occurs (curve 4 in Fig. 6). The phosphorescence reduces to $1/e$ of its peak value within 5.6 ns. In the $Ir(ppy)_3$ doped films (curves 2–4 in Fig. 7) the phosphorescence decay is non-exponential. It changes from an excitation intensity dependent fast initial decay to an approximately exponential decay of a time constant of about 1–2 μs. The excitation intensity dependence of the decay is seen by the curves 3 and 4. Both decay curves belong to 7.9 wt% of $Ir(ppy)_3$ in CBP, but for curve 4 (excitation energy density $w_{0L} \approx 5 \times 10^{-4}$ J cm^{-2}, $1/e$ decay time 28 ns) the excitation pulse energy density was approximately a factor of ten larger than for curve 3 (excitation energy density $w_{0L} \approx 5 \times 10^{-5}$ J cm^{-2}, $1/e$ decay time 130 ns).

Table 1
Spectroscopic parameters of $Ir(ppy)_3$ at room temperature

Parameter	Neat film	CBP	Polystyrene			THF as delivered	Chloroform as delivered	Toluene as delivered	Toluene de-aerated
Concentration		7.9 wt%	1 wt%	4 wt%	8 wt%	1.8×10^{-4} mol dm^{-3}	2.7×10^{-4} mol dm^{-3}	2.1×10^{-4} mol dm^{-3}	4.65×10^{-5} mol dm^{-3}
N_0 (cm^{-3})	2.1×10^{21}	$\approx7.6\times10^{19}$	9.7×10^{18}	3.9×10^{19}	7.7×10^{19}	1.08×10^{17}	1.6×10^{17}	1.27×10^{17}	2.8×10^{-16}
ϕ_P	0.0098 ± 0.0005	0.605 ± 0.04	0.915 ± 0.02	0.845 ± 0.02	0.82 ± 0.02	0.0195 ± 0.001	0.0177 ± 0.001	0.0162 ± 0.001	0.73 ± 0.06
n_A	1.755	1.796	1.606	1.606	1.606	1.4118	1.4522	1.5104	1.5104
n_P	1.72	1.794	1.596	1.596	1.596	1.4074	1.4476	1.5016	1.5016
d	65 nm	1.1 μm	10 μm	2.3 μm	1.2 μm	1 mm	1 mm	1 mm	15 mm
$\tau_P=\tau_T$ (ns)	15 ± 0.5	1200 ± 200	1200 ± 200	880 ± 150	1100 ± 200	25.7 ± 2	34.6 ± 2	23 ± 2	1090 ± 50
τ_{rad} (μs)	1.5 ± 0.05	2.0 ± 0.3	1.3 ± 0.2	1.0 ± 0.2	1.3 ± 0.2	1.32 ± 0.1	1.96 ± 0.1	1.5 ± 0.1	1.5 ± 0.1
$k_q[O_2]$ (s^{-1})						3.8×10^{7}	2.8×10^{7}	4×10^{7}	
Triplet–triplet annihilation results									
w_{0L} (J cm^{-2})		$\approx5\times10^{-5}$	3.2×10^{-5}	3.6×10^{-5}	4×10^{-5}				
$N_{T,ini,0}$ (cm^{-3})	$\approx6\times10^{-5}$	3.2×10^{17}	2.6×10^{16}	7.9×10^{16}	2.6×10^{17}				
$K_{T,0}$ (s^{-1})	1×10^{19}	2.6×10^{7}	1×10^{7}	5×10^{6}	8×10^{6}				
k_{TT} (cm^3 s^{-1})	6×10^{8}	1.6×10^{-10}	7.7×10^{-10}	1.3×10^{-10}	6.2×10^{-11}				
	$\approx1.2\times10^{-10}$								

4. Discussion

Structural, spectroscopic, and quantum chemical investigations identified the longest-wavelength absorption and the emission as a S_0–^{3}MLCT transition [29,32–34,37,50]. The spin–orbit coupling due to the heavy metal Ir makes the singlet to triplet absorption reasonably strong and allows the observation of phosphorescence at room temperature.

Recent time-dependent density functional theory on $Ir(ppy)_3$ revealed the presence of three lowest triplet states of nearly equal energy ($\lambda\approx480$ nm) [37]. The thin triple-dotted curve in Fig. 4 shows the absorption cross-section spectrum due to the transition from the ground state to one of these three triplet states, T_1. Assuming the same oscillator strength for the transition from the ground-state to the two other triplet states, T_2 and T_3, then we obtain the absorption cross-section spectrum shown by the thick triple-dotted curve in Fig. 4 belonging to T_1, T_2, and T_3. The total long-wavelength singlet to triplet absorption cross-section around 480 nm approaches the experimentally measured long-wavelength absorption cross-section around 480 nm. The open-circle line in Fig. 4 shows the absorption cross-section of $Ir(ppy)_3$ in THF without the expected S_0–^{3}MLCT contribution.

The phosphorescence quantum yield of $Ir(ppy)_3$ doped in polystyrene and in CBP films was found to be very high ($\phi_P=60$–90%). At the applied concentrations of up to 8 wt% the concentration quenching is still weak. A reduction of the phosphorescence quantum yield from $\phi_P(1\text{ wt}\%)=0.915$ to $\phi_P(8\text{ wt}\%)=0.82$ is observed in the case of $Ir(ppy)_3$ in polystyrene. There is no severe triplet quenching by oxygen because of the immobilization of the dissolved oxygen in the solid films (polystyrene is not permeable to oxygen [51]). The phosphorescence quantum yield of the neat $Ir(ppy)_3$ film turned out to be rather low ($\phi_P\approx0.01$). There occurs a strong self-quenching. Also the phosphorescence spectrum has a different shape. Maybe some kind of aggregation occurs which opens non-radiative decay channels.

Our results on the photoluminescence of 7.9 wt% $Ir(ppy)_3$ in CBP compare well with electroluminescence (EL) results obtained with OLEDs based $Ir(ppy)_3$ in CBP [4,36]. In [4] external electroluminescence quantum efficiencies of =0.05, 0.08, and 0.03 are reported for 1 wt%, 6 wt%, and 12 wt% of $Ir(ppy)_3$ in CBP, respectively. For an OLED with a neat 100% $Ir(ppy)_3$ layer the external quantum efficiency reduced to $\phi_{EL,ext}=0.007$ [4]. In [36] an external EL quantum efficiency of $\phi_{EL,ext}=0.090$ is obtained for an OLED based on 7 wt% of $Ir(ppy)_3$ in CBP using a MgAg cathode. The internal EL quantum efficiency, $\phi_{EL,int}$, is thought to be approximately five times larger than the external EL quantum efficiency, $\phi_{EL,ext}$ [4]. The obtained effi-

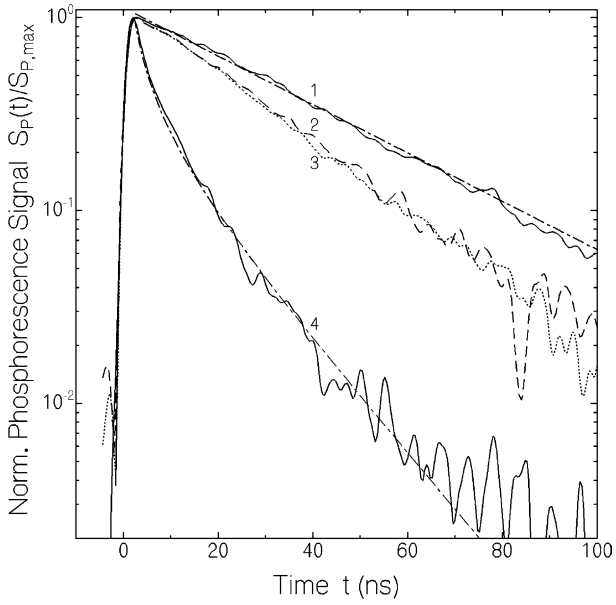

Fig. 6. Phosphorescence signal traces of $Ir(ppy)_3$. Curve 1: solvent is chloroform with single exponential fit (dash-dotted curve, $\tau_P = 34.6$ ns). Curve 2 (dashed): solvent is THF ($\tau_P = 25.7$ ns). Curve 3 (dotted): solvent is toluene ($\tau_P = 24.7$ ns). Curve 4: neat film, excitation peak energy density $w_{0L} \approx 6 \times 10^{-5}$ J cm^{-2} causing peak initial triplet population number density $N_{T,ini,0} \approx 1 \times 10^{19}$ cm^{-3}. The triplet–triplet annihilation fit (Eq. (13), dash-dotted curve) gives $K_{T,0} = 6 \times 10^8$ s^{-1} and $\tau_T = 15$ ns leading to $k_{TT} \approx 1.2 \times 10^{-10}$ cm^3 s^{-1}.

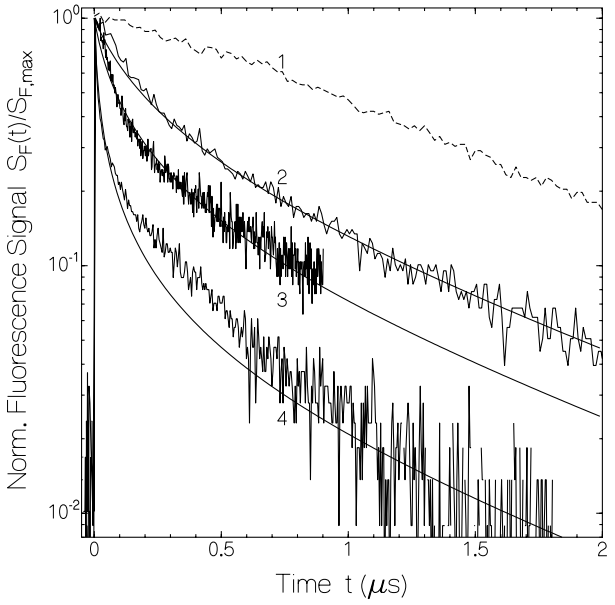

Fig. 7. Temporal phosphorescence traces. Film parameters are given in Table 1. Curve 1: $Ir(ppy)_3$ in de-areated toluene at 25.6 °C. Curves 2: 1 wt% $Ir(ppy)_3$ in polystyrene; peak excitation energy density, $w_{0L} \approx 3.2 \times 10^{-5}$ J cm^{-2} giving initial triplet population $N_{T,ini,0} \approx 2.6 \times 10^{16}$ cm^{-3}; fit parameters (Eq. (13)) are $\tau_T = 1.2$ μs and $K_{T,0} = 1 \times 10^7$ s^{-1} leading to $k_{TT} \approx 7.7 \times 10^{-10}$ cm^3 s^{-1}. Curves 3: 7.9 wt% $Ir(ppy)_3$ in CBP; $w_{0L} \approx 5 \times 10^{-5}$ J cm^{-2} giving $N_{T,ini,0} \approx 3.2 \times 10^{17}$ cm^{-3}; fit parameters: $\tau_T = 1.2$ μs and $K_{T,0} = 2.6 \times 10^7$ s^{-1} leading to $k_{TT} \approx 1.6 \times 10^{-10}$ cm^3 s^{-1}. Curves 4: 7.9 wt% $Ir(ppy)_3$ in CBP; $w_{0L} \approx 5 \times 10^{-4}$ J cm^{-2} giving $N_{T,ini,0} \approx 3.2 \times 10^{18}$ cm^{-3}; fit parameters: $\tau_T = 1.2$ μs and $K_{T,0} = 1.4 \times 10^8$ s^{-1} leading to $k_{TT} \approx 8.8 \times 10^{-11}$ cm^3 s^{-1}.

ciency of $\phi_{EL,int} \approx 0.45$ for 7 wt% $Ir(ppy)_3$ in CBP [36] compares well with our internal photoluminescence efficiency of $\phi_P \approx 0.60$ for 7.9 wt% $Ir(ppy)_3$ in CBP.

The phosphorescence quantum yield of $Ir(ppy)_3$ in de-aerated toluene is determined to be $\phi_P \approx 0.73$. The phosphorescence quantum yield of $Ir(ppy)_3$ in the studied air-saturated organic solutions was in the range of 1.5–2% (see Table 1). These small phosphorescence quantum yields are due to triplet oxygen quenching. The phosphorescence quantum yield in the case of oxygen quenching is approximately given by [52]

$$\phi_P = \frac{\tau_{rad}^{-1}}{\tau_{rad}^{-1} + k_{nr,0} + k_q[O_2]} \approx \frac{\tau_{rad}^{-1}}{\tau_{rad}^{-1} + k_q[O_2]} = \frac{1}{1 + \tau_{rad} k_q [O_2]}, \quad (3)$$

where $k_{nr,0}$ is the non-radiative rate constant in the absence of oxygen, k_q is the bimolecular reaction coefficient, and $[O_2]$ is the concentration of dissolved oxygen. The oxygen quenching rate is

$$k_q[O_2] \approx \frac{1 - \phi_P}{\phi_P \tau_{rad}} = \frac{1 - \phi_P}{\tau_P}. \quad (4)$$

Values of $k_q[O_2]$ are included in Table 1.

The quenching of the phosphorescence of $Ir(ppy)_3$ immobilized in oxygen-permeable poly(styrene-co-2,2,2-trifluoroethyl methacrylate) films by oxygen is applied for oxygen sensing [51]. A similar oxygen-sensitive decrease of phosphorescence was observed for PtOEP in oxygen-permeable poly(isobutylmethacrylate-co-trifluoroethylmethacrylate) films [53].

The temporal phosphorescence signal measurements were carried out by picosecond laser pulse singlet–singlet excitation. The excitation is transferred to the lowest triplet state by excited-state internal conversion and intersystem crossing. The quantum yield of triplet formation is thought to be practically 100% since no indication of fluorescence emission is observed (emission from lowest ^{1}MLCT singlet state would result in emission down to 460 nm with short fluorescence lifetime).

For the low-concentration air-saturated liquid solutions (approximately 2×10^{-4} M, see Table 1) single-exponential phosphorescence decay in the 23 ns to 35 ns time region is observed. There no triplet–triplet annihilation is observed since the triplet lifetime is short and the average molecular separation is large (low concentration, molecular separation $d_s \approx N_0^{-1/3} = (CN_A/1000)^{-1/3} \approx 20$ nm, where N_0 is the $Ir(ppy)_3$ number density, C is the $Ir(ppy)_3$ concentration in mol dm^{-3}, and N_A is the Avogadro constant).

For the neat film non-exponential phosphorescence decay is observed despite the strong self-quenching (low quantum yield, low over-all lifetime) because the

picosecond pulse excitation (pulse energy density $w_L \approx 6\times10^{-5}$ J cm^{-2}) leads to nearby excitation of triplet molecules which quench by triplet–triplet annihilation (average separation between two excited triplet molecules is $d_T \approx N_T^{-1/3} \approx (w_L\alpha_L/hv_L)^{-1/3} \approx 4.8$ nm, where α_L is the absorption coefficient at the laser frequency v_L, and h is the Planck constant). Additionally energy transfer between excited molecules and neighbouring unexcited molecules may bring two excited molecules together for annihilation. In the Ir(ppy)$_3$ doped films the dye density is high (e.g., number density $N_{dop} = \rho w_{\%}/(100M_m)N_A \approx 9.7\times10^{18}$ cm^{-3} for $w_{\%} = 1$ wt% of Ir(ppy)$_3$ in polystyrene of mass density $\rho = 1.05$ g cm^{-3}, and molar mass $M_m = 654.79$ g mol^{-1} of Ir(ppy)$_3$) and therefore the average nearest neighbour distance is small (≈4.7 nm for selected example). Therefore under intense picosecond pulse excitation, the excitation of near-distant molecules occurs ($d_T \approx N_T^{-1/3} \approx (w_L N_{dop}\sigma_{a,L}/hv_L)^{-1/3}$, where $\sigma_{a,L}$ is the Ir(ppy)$_3$ absorption cross-section at the excitation laser wavelength), and the excitation migrates due to energy transfer. Two nearby excited molecules decay by triplet–triplet annihilation.

The dynamics of triplet–triplet annihilation in organometallic compounds is described in detail in [15]. After picosecond pulse excitation the excited electrons are accumulated in the ^{3}MLCT triplet state, ^{3}M*. Two nearby excited molecules interact by transferring one molecule to a higher excited state and transferring the other molecule to the singlet ground-state, M. The higher excited state molecule relaxes back non-radiatively to the initial triplet state, thereby one excitation is annihilated. The overall annihilation reaction is

$$^3M^* + {}^3M^* \xrightarrow{k_{TT}} {}^3M^* + M \tag{5}$$

where k_{TT} is the triplet–triplet annihilation constant. The triplet state number density, N_T decays due to radiative and non-radiative triplet–singlet relaxation (triplet state lifetime τ_T equal to phosphorescence time constant τ_P), and due to triplet–triplet annihilation according to

$$\frac{dN_T}{dt} = -\frac{N_T}{\tau_T} - \frac{1}{2}k_{TT}N_T^2. \tag{6}$$

The solution of this Riccati differential equation with the initial condition, $N_T(0) = N_{T,0}$ is [15]

$$N_T(t) = \frac{N_{T,ini}}{(1+K_T\tau_T)\exp(t/\tau_T) - K_T\tau_T}, \tag{7}$$

with

$$K_T = \frac{1}{2}k_{TT}N_{T,ini}. \tag{8}$$

The initial triplet population number density, $N_{T,ini}$ is estimated from the pump laser excitation energy density, w_L by the relation [54]

$$N_{T,ini} = \frac{N_0 w_L/w_s}{1 + w_L/w_s}, \tag{9}$$

where $w_s = hv_L/\sigma_{a,L}$ is the saturation energy density ($w_s = 0.0124$ J cm^{-2} for $\lambda_L = 347.15$ nm and $\sigma_{a,L} = 4.6\times10^{-17}$ cm^2). h is the Planck constant, $v_L = c_0/\lambda_L$ is the pump laser frequency, $\sigma_{a,L}$ is the absorption cross-section at the laser frequency, and N_0 is the number density of Ir(ppy)$_3$ molecules. N_0 values are included in Table 1. Eq. (9) simplifies to

$$N_{T,ini} = \frac{N_0\sigma_{a,L}w_L}{hv_L}, \tag{10}$$

for $w_L < w_s$ Experimental values of peak input energy density, w_{0L} and calculated peak triplet population number density values, $N_{T,ini,0}$ are given in the figure captions of Figs. 6 and 7 and in Table 1.

The phosphorescence intensity, $I_P(r,t)$, is proportional to the triplet population, $N_T(r,t)$, where r is the cross-sectional coordinate. Therefore the phosphorescence intensity is expected to be

$$I_P(r,t) = \frac{\kappa N_{T,ini}(r)}{[1+K_T(r)\tau_T]\exp(t/\tau_T) - K_T(r)\tau_T}. \tag{11}$$

Assuming a Gaussian energy density distribution, $w_L(r) = w_{0L}\exp(-r^2/r_{0L}^2)$, for $w_{0L} < w_s$ the phosphorescence power, $S_P(t)$, is given by

$$S_P(t) = \int_0^\infty \frac{\kappa N_{T,ini,0}\exp(-r^2/r_{0L}^2)}{[1+K_{T,0}\exp(-r^2/r_{0L}^2)\tau_T]\exp(t/\tau_T) - K_{T,0}\exp(-r^2/r_{0L}^2)\tau_T} 2\pi r\,dr, \tag{12}$$

and the normalized phosphorescence power, $S_P(t)/S_P(0)$, is with

$$S_P(t)/S_P(0) = 2\int_0^\infty \frac{\exp(-r^2)}{[1+K_{T,0}\exp(-r^2)\tau_T]\exp(t/\tau_T) - K_{T,0}\exp(-r^2)\tau_T} r\,dr, \tag{13}$$

$$K_{T,0} = \frac{1}{2} k_{TT} N_{T,ini,0} = \frac{1}{2} k_{TT} \frac{N_0 w_{0L}/w_s}{1 + w_L/w_s}. \quad (14)$$

The non-exponential phosphorescence signal decays in Figs. 6 and 7 are fitted by Eq. (13). The fit parameters, $K_{T,0}$ are listed in the figure captions and in Table 1. The obtained triplet–triplet annihilation constants, k_{TT} are listed in Table 1.

Our phosphorescence lifetime and phosphorescence quantum yield measurements lead to a ^{3}MLCT $\rightarrow S_0$ radiative lifetime of τ_{rad} 1–2 μs for Ir(ppy)$_3$ in neat film, solid solution and liquid solution at room temperature (see Table 1). In [30] a luminescence lifetime of $\tau_P \approx 2$ μs and a luminescence quantum yield of $\phi_P \approx 0.4$ were reported for Ir(ppy)$_3$ in de-aerated toluene at room temperature leading to $\tau_{rad} \approx 5$ μs. We determine $\tau_P \approx 1.1$ μs and $\phi_P \approx 0.73$ giving $\tau_{rad} \approx 1.5$ μs. The origin of this difference is not known at presence. Phosphorescence lifetimes of $\tau_P = 1.9$ and 2 μs are given in [28] and [30] for Ir(ppy)$_3$ in de-aerated acetonitrile and degassed toluene, respectively, at room temperature.

A strong temperature dependence of the phosphorescence lifetime was observed for Ir(ppy)$_3$ in THF in a temperature range from 1.2 to 135 K [34]. The lifetime was observed to increase with decreasing temperature (e.g., $\tau_P = 2$ μs at 135 K, and $\tau_P = 145$ μs at 1.2 K [34]). The lifetime at 135 K was found to be almost the same as at room temperature. In ref. [34] it is shown that the triplet degeneracy is lifted to three sublevels (zero-field splitting) with different singlet–triplet oscillator strengths. The temperature dependence of the phosphorescence lifetime is explained by the temperature dependent Boltzmann level population distribution (radiative lifetimes of the three sublevels: 145, 11, and 750 ns). It is suggested that the radiative lifetime of the upper sublevel is mainly responsible for the phosphorescence lifetime at room temperature.

In films of fluorescent organic molecules [55,56] and polymers [57] wave-guided amplification of spontaneous emission (travelling-wave lasing) [58] and feed-back laser action [59,60] has been observed (for reviews see [57,61–64]). Here intense transverse picosecond laser pumping of a 2 μm thick film consisting of 4 wt% Ir(ppy)$_3$ in polystyrene (excitation wavelength $\lambda_L = 347.15$ nm, pulse duration $\Delta t_L = 35$ ps, excitation energy density up to $w_{0L} = 1.2 \times 10^{-2}$ J cm^{-2}, pumped film area 0.2 mm × 5 mm) gave no indication of amplified spontaneous emission which should have shown up in a spectral narrowing of the edge-emitted triplet emission spectrum (in direction of line focus where amplification length is longest [58]). The maximum amplification of spontaneous emission, $G(\lambda) = S_{ASE}(\lambda)/S_P(\lambda)$, is approximately given by [58]

$$G(\lambda) = \exp[N_{T,ini,0}\sigma_{em,eff}(\lambda)\ell'] = \exp\left[\frac{N_0 w_{0L}/w_s}{1 + w_{0L}/w_s}\sigma_{em,eff}(\lambda)\ell'\right], \quad (15)$$

where $\sigma_{em,eff}(\lambda) = \sigma_{em}(\lambda) - \sigma_{ex}(\lambda)$ is the effective stimulated emission cross-section, $\sigma_{ex}(\lambda)$ is the excited-state absorption cross-section, and ℓ' is the effective gain length ($\leqslant$ pumped length because of ground-state re-absorption and scattering losses). Neglecting excited-state absorption, ground-state re-absorption and scattering losses a maximum gain factor of $G_{max} \approx 50$ is estimated using $w_{0L} = 0.01$ J cm^{-2}, $N_0 \approx 3.9 \times 10^{19}$ cm^{-3}, $w_s = 1.2 \times 10^{-2}$ J cm^{-2}, $\sigma_{em,max} = 4 \times 10^{-19}$ cm^2, and $\ell' = 0.5$ cm. The non-observation of light amplification indicates that the excited-state absorption is equal or larger than the stimulated emission cross-section and/or the effective gain length is small compared to the pumped sample length. In [31] the excited-state absorption cross-section spectrum of Ir(ppy)$_3$ is given. From there a value of $\sigma_{ex} \approx 2.5 \times 10^{-18}$ cm^2 is extracted at the wavelength position of maximum stimulated emission cross-section ($\lambda_{max} \approx 540$ nm). Since this value is larger than the maximum stimulated emission cross-section of $\sigma_{em,max} \approx 4 \times 10^{-19}$ cm^2, no amplified spontaneous emission should occur in agreement with the experimental findings.

5. Conclusions

In this paper the absorption and emission spectroscopic behaviour of the metal-organic complex Ir(ppy)$_3$ in three organic solvents (chloroform, toluene, and tetrahydrofuran), doped in organic films (polystyrene and CBP), and as neat film on a quartz plate has been studied. The enhancement of spin–orbit coupling by the heavy metal Ir causes measurable long-wavelength S_0–^{3}MLCT singlet triplet absorption, practically 100% excited-state singlet–triplet intersystem crossing, and high-efficient phosphorescence in doped films at room temperature (phosphorescence quantum yield up to 90%). In neat films the phosphorescence quantum yield is reduced to about 1% by self-quenching probably due to aggregation. In air-saturated liquid solution oxygen quenching reduces the phosphorescence quantum efficiency to the 2% region.

The T_1(^{3}MLCT)–S_0 stimulated emission cross-section spectrum has been extracted from the phosphorescence quantum distribution. Mirror symmetry arguments between the emission spectrum and the absorption spectrum together with the Einstein coefficient relations between absorption and emission of a transition have been applied to reveal the S_0–T_1(^{3}MLCT) absorption cross-section spectrum centred at around 470 nm from the total absorption cross-section spectrum.

Under short-pulse laser excitation conditions in heavily doped films the phosphorescence efficiency is reduced and the phosphorescence lifetime is shortened by triplet–triplet annihilation. This annihilation may affect the OLED performance in nanosecond pulse applications. Laser action of $Ir(ppy)_3$ doped films was not achieved at room temperature. The excited-state-absorption cross-section in the triplet system is reportedly higher than the triplet–singlet stimulated emission cross-section in the phosphorescence wavelength region at room temperature and therefore laser action is not expected.

Acknowledgement

We sincerely thank the Corporate R&D Laboratories, Pioneer Corporation, Japan for kindly providing the $Ir(ppy)_3$ neat film evaporated on quartz plate, and we thank Anja Merkel for technical assistance. One of the authors (TT) is indebted to the Japan Society for Promotion of Science for a partial support by the Grant-in-Aid for Scientific Research (C, Project No.15550165).

References

[1] H. Xin, F.Y. Li, M. Guan, C.H. Huang, M. Sun, K.Z. Wang, Y.A. Zhang, L.P. Jin, J. Appl. Phys. 94 (2003) 4729.
[2] S. Hoshino, H. Suzuki, Appl. Phys. Lett. 69 (1996) 224.
[3] Y. Ma, C.-M. Che, H.-Y. Chao, X. Xhou, W.-H. Chau, J. Shen, Adv. Mater. 11 (1989) 852.
[4] M.A. Baldo, M.E. Thompson, S.R. Forrest, Pure Appl. Chem. 71 (1999) 2095.
[5] V. Cleave, G. Yahioglu, P.L. Barny, R.H. Friend, N. Tessler, Adv. Mater. 11 (1999) 285.
[6] R.W.T. Higgins, A.P. Monkman, H.-G. Nothofer, U. Scherf, J. Appl. Phys. 91 (2002) 99.
[7] D.F. O'Brien, C. Giebeler, R.B. Fletcher, A.J. Cadby, L.C. Palilis, D.G. Lidzey, P.A. Lane, D.D.C. Bradley, W. Blau, Synth. Met. 116 (2001) 379.
[8] P.A. Lane, L.C. Palilis, D.F. O'Brien, C. Giebeler, A.J. Cadby, D.G. Lidzey, A.J. Campbell, W. Blau, D.D.C. Bradley, Phys. Rev. B 63 (2001) 235206.
[9] D.F. O'Brien, M.A. Baldo, M.E. Thompson, S.R. Forrest, Appl. Phys. Lett. 74 (1999) 442.
[10] M.A. Baldo, D.F. O'Brien, Y. You, A. Shoustikov, S. Silbey, M.E. Thompson, S.R. Forrest, Nature 395 (1998) 151.
[11] M.A. Baldo, S. Lamansky, P.E. Burrows, M.E. Thompson, S.R. Forrest, Appl. Phys. Lett. 75 (1999) 4.
[12] T. Watanabe, K. Nakamura, S. Kawami, Y. Fukuda, T. Tsuji, T. Wakimoto, S. Miyaguchi, SPIE 4105 (2001) 175.
[13] M.J. Yang, T. Tsutsui, Jpn. J. Appl. Phys. A 39 (8A) (2000) L828, Part 2.
[14] Y. Kawamura, S. Yanagida, S.R. Forrest, J. Appl. Phys. 92 (2002) 87.
[15] M.A. Baldo, C. Adachi, S.R. Forrest, Phys. Rev. B 62 (2000) 10967.
[16] S. Lamansky, P. Djurovich, D. Murphy, F. Abdel-Razzaq, H.-E. Lee, C. Adachi, P.E. Burrows, S.R. Forrest, M.E. Thompson, J. Am. Chem. Soc. 123 (2001) 4304.
[17] R.R. Das, C.-L. Lee, J.-J. Kim, Mat. Res. Soc. Symp. Proc. 708 (2002) BB3.39.1.
[18] X. Gong, J.C. Ostrowski, D. Moses, G.C. Guillermo, C. Bazan, A.J. Heeger, Adv. Funct. Mater. 13 (2003) 439.
[19] X. Gong, J.C. Ostrowski, D. Moses, G.C. Guillermo, C. Bazan, A.J. Heeger, J. Polym. Sci. Part B: Polym. Phys. 41 (2003) 2691.
[20] F. Shen, H. Xia, C. Zhang, D. Lin, X. Liu, Y. Ma, Appl. Phys. Lett. 84 (2004) 55.
[21] A. Nakamura, T. Tada, M. Mizukami, S. Yagyu, Appl. Phys. Lett. 84 (2004) 130.
[22] M. Ikai, S. Tokito, Y. Sakamoto, T. Suzuki, Y. Taga, Appl. Phys. Lett. 79 (2001) 156.
[23] M.A. Baldo, M.E. Thompson, S.R. Forrest, Nature 403 (2000) 750.
[24] R.C. Kwong, S. Lamansky, M.E. Thompson, Adv. Mater. 12 (2000) 1134.
[25] C.-L. Lee, K.B. Lee, J.-J. Kim, Appl. Phys. Lett. 77 (2000) 2280.
[26] G. Ramos-Ortiz, Y. Oki, B. Domercq, B. Kippelen, Phys. Chem. Chem. Phys. 4 (2002) 4109.
[27] M.A. Baldo, S.R. Forrest, Phys. Rev. 62 (2000) 10958.
[28] K. Dedeian, P.I. Djurovich, F.O. Garces, G. Carlson, R.J. Watts, Inorg. Chem. 30 (1991) 1687.
[29] M.G. Colombo, T.C. Brunold, T. Riedener, H.U. Güdel, M. Förtsch, H.-B. Bürgi, Inorg. Chem. 33 (1994) 545.
[30] K.A. King, P.J. Spellane, R.J. Watts, J. Am. Chem. Soc. 107 (1985) 1431.
[31] K. Ichimura, T. Kobayashi, K.A. King, R.J. Watts, J. Phys. Chem. 91 (1987) 6104.
[32] A. Tsuboyama, H. Iwawaki, M. Furugori, T. Mukaide, J. Kamatani, S. Igawa, T. Moriyama, S. Miura, T. Takiguchi, S. Okada, M. Hoshino, K. Ueno, J. Am. Chem. Soc. 125 (2003) 12971.
[33] T. Tsuboi, M. Tanigawa, Thin Solid Films 438–439 (2003) 301.
[34] W. Finkenzeller, H. Yersin, Chem. Phys. Lett. 377 (2003) 299.
[35] A. Tsuboyama, T. Takiguchi, S. Okada, M. Osawa, M. Hoshino, K. Ueno, Dalton Trans. (2004) 1115.
[36] C. Adachi, M.A. Baldo, S.R. Forrest, M.E. Thompson, Appl. Phys. Lett. 77 (2000) 904.
[37] P.J. Hay, J. Phys. Chem. A 106 (2002) 1634.
[38] A. Penzkofer, E. Drotleff, W. Holzer, Opt. Commun. 158 (1998) 221.
[39] W. Holzer, M. Pichlmaier, A. Penzkofer, D.D.C. Bradley, W.J. Blau, Opt. Commun. 163 (1999) 24.
[40] A. Penzkofer, W. Holzer, H. Tillmann, H.H. Hörhold, Opt. Commun. 229 (2004) 279.
[41] A. Penzkofer, W. Leupacher, J. Lumin. 37 (1987) 61.
[42] W. Holzer, M. Pichlmaier, A. Penzkofer, D.D.C. Bradley, W.J. Blau, Chem. Phys. 246 (1999) 445.
[43] W.H. Melhuish, J. Phys. Chem. 65 (1961) 229.
[44] P. Weidner, A. Penzkofer, Opt. Quant. Electron. 25 (1993) 1.
[45] O.G. Peterson, J.P. Webb, W.C. McColgin, J.H. Eberly, J. Appl. Phys. 42 (1971) 1917.
[46] A.V. Deshpande, A. Beidoun, A. Penzkofer, G. Wagenblast, Chem. Phys. 142 (1990) 123.
[47] S.J. Strickler, R.A. Berg, J. Chem. Phys. 37 (1962) 814.
[48] J.B. Birks, D.J. Dyson, Proc. R. Soc. Lond. A 275 (1963) 135.
[49] W. Demtöder, Laser Spectroscopy. Basic Concepts and Instrumentation, Springer Series in Chemical Physics, vol. 5, Springer-Verlag, Berlin, 1981.
[50] S. Sprouse, K.A. King, P.J. Spellane, R.J. Watts, J. Am. Chem. Soc. 106 (1984) 6647.
[51] Y. Amano, Y. Ishikawa, I. Okura, Anal. Chim. Acta 445 (2001) 177.
[52] B. Valeur, Molecular Fluorescence. Principles and Applications, Wiley-VHC, Weinheim, 2002.
[53] Y. Amano, T. Miyashita, I. Okura, Anal. Chim. Acta 421 (2000) 167.
[54] M. Hercher, Appl. Opt. 6 (1967) 947.

[55] J. Salbeck, M. Schörner, T. Fuhrmann, Thin Solid Films 417 (2002) 20.
[56] R. Philip, W. Holzer, A. Penzkofer, H. Tillmann, H.-H. Hörhold, Synth. Met. 132 (2003) 297.
[57] M.D. McGehee, A.J. Heeger, Adv. Mater. 12 (2000) 1655.
[58] W. Holzer, A. Penzkofer, T. Schmitt, A. Hartmann, C. Bader, H. Tillmann, D. Raabe, R. Stockmann, H.-H. Hörhold, Opt. Quant. Electron. 33 (2001) 121.
[59] G.J. Denton, N. Tessler, M.A. Stevens, R.H. Friend, Adv. Mater. 9 (1997) 547.
[60] W. Holzer, A. Penzkofer, T. Pertsch, N. Danz, A. Bräuer, E.B. Kley, H. Tillmann, C. Bader, H.-H. Hörhold, Appl. Phys. B 74 (2002) 333.
[61] U. Lemmer, A. Haugeneder, C. Kallinger, J. Feldmann, in: P. van Hutten (Ed.), Semiconducting Polymers: Chemistry, Physics and Engineering, Wiley-VCH, Weinheim, 1999, p. 309.
[62] S.V. Frolov, M. Shkunov, A. Fujii, K. Yosino, Z.V. Vardeny, IEEE J. Quantum Electron. 36 (2000) 2.
[63] G. Kranzelbinder, G. Leising, Rep. Prog. Phys. 63 (2000) 729.
[64] U. Scherf, S. Riechel, U. Lemmer, R.F. Mahrt, Curr. Opin. Solid State Mater. Sci. 5 (2001) 143.